第 27 卷第 4 期 无 机 化 学 学 报 Vol.27 No.4
2011 年 4 月 CHINESE JOURNAL OF INORGANIC CHEMISTRY 776-780

Li^+共掺杂对 Er^{3+}-Yb^{3+}:TiO_2 紫外、可见和红外发光同步增强研究

曹保胜[1,2] 何洋洋[3] 冯志庆[1] 宋 苗[1] 董 斌*,[1]
([1]大连民族学院理学院,大连 116600)
([2]中科院长春应用化学研究所高分子物理与化学国家重点实验室,长春 130022)
([3]杜伊斯堡–埃森大学物理系,杜伊斯堡 47057,德国)

摘要:采用溶胶–凝胶(Sol-gel)法制备了 Li^+共掺杂的 Er^{3+}-Yb^{3+}:TiO_2 粉末。976 nm 激光激发下在波长 350~1700 nm 范围内观察到了紫外、蓝色、绿色和红色上转换发光和红外下转换发光。随着 Li^+共掺杂浓度由 0 增大到 20mol%,Er^{3+}-Yb^{3+}:TiO_2 的紫外、可见和红外发光强度同步增强。低 Li^+共掺杂浓度引起的 Li^+固溶以及高 Li^+共掺杂浓度引起的相变过程相继破坏了 Er^{3+}的晶体场对称性,导致紫外、可见和红外发光显著增强。结果表明共掺杂 Li^+是一种提高 Er^{3+}掺杂材料发光性能的有效方法。

关键词:Er^{3+}-Yb^{3+}:TiO_2; Li^+共掺杂; 紫外、可见和红外发光; 晶体场对称性
中图分类号:TQ134.1+1 **文献标识码**:A **文章编号**:1001-4861(2011)04-0776-05

Simultaneous Enhanced Ultraviolet, Visible and Infrared Emissions in Er^{3+}-Yb^{3+}:TiO_2 by Li^+ Codoping

CAO Bao-Sheng[1,2] HE Yang-Yang[3] FENG Zhi-Qing[1] SONG Miao[1] DONG Bin*,[1]
([1]*School of Science, Dalian Nationalities University, Dalian, Liaoning* 116600, *China*)
([2]*State Key Laboratory of Polymer Physics and Chemistry, Changchun Institute of Applied Chemistry, Chinese Academy of Sciences, Changchun* 130022, *China*)
([3]*Faculty of Physics, University Duisburg-Essen, Duisburg* 47057, *Germany*)

Abstract: The Er^{3+}-Yb^{3+}:TiO_2 powders by Li^+ codoping have been prepared by sol-gel method. Both ultraviolet, blue, green and red upconversion and infrared downconversion emissions in the wavelengths of 350~1 700 nm were observed by a 976 nm semiconductor laser diode (LD) excitation. The ultraviolet, visible and infrared emissions of Er^{3+}-Yb^{3+}:TiO_2 enhanced simultaneously by increasing Li^+ from 0 to 20mol%. The significant enhancement of ultraviolet, visible and infrared emissions resulted from the distortion of crystal field symmetry of Er^{3+} caused by the dissolving of Li^+ at lower Li^+ codoping concentration and the phase transformation at higher Li^+ concentration. It can be concluded that codoping with Li^+ is an efficient method to enhance the luminescence of Er^{3+} doped materials.

Key words: Er^{3+}-Yb^{3+}:TiO_2; Li^+ codoping; ultraviolet, visible and infrared emissions; crystal field symmetry

Rare-earth ions doped luminescence materials have attracted much attention because of the application to color display, data storage, biological diagnosis, infrared detection and temperature sensor[1-5]. Er^{3+} is one of the most popular rear-earth ions due to its upconversion and downconversion emissions in Er^{3+} doped luminescence materials under the excitation of 980 nm semiconductor laser diodes (LD). However, the relative low absorption cross-section of Er^{3+} at 980 nm limits the efficiency of Er^{3+}. It is well-known that the

收稿日期:2010-11-22。收修改稿日期:2010-12-12。
国家自然科学基金(No.11004021,10804015);中央高校基本科研业务费专项资金(No.DC10040122)资助项目。
*通讯联系人。E-mail:dong@dlnu.edu.cn

luminescence efficiency of Er^{3+} doped materials is dependent on their intra 4*f* transition probabilities[6-8]. The intra 4*f* transition probabilities of Er^{3+} in Er^{3+} doped materials are related to the energy migration between active ions and the crystal field symmetry of active ions in the host matrix[9-10]. Codoping with Yb^{3+} is an efficient method to overcome the low absorption cross-section of Er^{3+} because of the larger absorption cross-section of Yb^{3+} at 980 nm and the large spectral overlap between Yb^{3+} emission and Er^{3+} absorption which results in an efficient resonant energy migration from Yb^{3+} to Er^{3+}[11-13]. On the other hand, the change of crystal field symmetry of Er^{3+} can also affect the intra 4*f* transition probabilities of Er^{3+}. Patra et al.[9] found that the green and red upconversion emissions intensities of Er^{3+}:ZrO_2 nanocrystals depended on their phase structures. Compared with tetragonal phase, the monoclinic phase of ZrO_2 with lower crystal field symmetry was more favorable to the green and red emissions of Er^{3+}:ZrO_2 nanocrystals. For the Er^{3+}:TiO_2 nanocrystals, the mixture of rutile and anatase phases with the lowest crystal field symmetry caused the maximum green and red upconversion emissions intensities[10]. The dopant of Li^+ with small ionic radius can change the luminescence emissions of Er^{3+} after introduced into the Er^{3+} doped luminescence materials[14]. Bai et al.[15-16] and Chen et al.[17-18] reported that the formation of Li^+ solution by Li^+ codoping could enhance the upconversion emissions intensities of Er^{3+}:Y_2O_3 and ZnO nanocrystals due to the distortion of crystal field symmetry of Er^{3+}. In this paper, we report that both Li^+ solution and the phase transformation caused by Li^+ codoping can simultaneously enhance the ultraviolet, visible upconversion and infrared downconversion emissions of Er^{3+} in the Er^{3+}-Yb^{3+}:TiO_2 powders by Li^+ codoping, also the corresponding mechanism is discussed.

1 Experimental

Sol-gel method was used to prepare the Er^{3+}-Yb^{3+}-Li^+ codoped TiO_2 powders. The iso-propyl (*i*-PrOH) was first added as solvent into the modified titanium(Ⅳ) *n*-butoxide which was performed by chelating reaction between *n*-butyl titanate ($Ti(OBu)_4$) and acetylacetone (AcAc) under agitation for 1 h at room temperature. Then a mixture of deionized water, *i*-PrOH and the concentrated nitric acid (HNO_3) were added slowly into the solution. The mixed solution was stirred for 6 h to form a clear and stable TiO_2 sol. The molar ratios of $Ti(OBu)_4$ to AcAc, H_2O and HNO_3 were 1∶1, 1∶2 and 3∶1, respectively. Finally, Er^{3+}, Yb^{3+} and Li^+ were introduced by adding $Er(NO_3)_3\cdot 5H_2O$, $Yb(NO_3)_3\cdot 5H_2O$ and $LiNO_3$ in the molar ratio of 1∶10∶(0~20)∶100 for Er^{3+}∶Yb^{3+}∶Li^+∶Ti^{4+}. The Er^{3+}-Yb^{3+}-Li^+ codoped TiO_2 sols were dried at 100 ℃ for 8 h to get rid of the solvent. The xerogels obtained were heated at the heating rate of 4 ℃·min^{-1} and kept at the sintering temperature of 1 250 ℃ for 1 h, and then cooled down to room temperature in the furnace. The doped TiO_2 sintered was milled into powder for structural analysis and spectral measurement.

The phase structures of the Er^{3+}-Yb^{3+}-Li^+ codoped TiO_2 powders were analyzed by SHIMADZU XRD-6000 X-ray diffractormeter (XRD) with Cu *Kα* radiation. The luminescence emissions spectra were obtained by a 976 nm semiconductor LD excitation. The luminescence emissions from the powders were focused onto Jobin Yvon iHr550 monochromator and detected with CR131 photomultiplier tube and InGaAs detector associated with a lock-in amplifier. The spectral resolution of the experimental set-up was 0.1 nm. All the spectroscopic measurements were carried out at room temperature.

2 Results and discussion

Fig.1 shows the XRD patterns of 1mol% Er^{3+}-10mol% Yb^{3+} doped TiO_2 by 0mol%~20mol% Li^+ codoping. The XRD pattern of Er^{3+}-Yb^{3+}:TiO_2 is characteristic of tetragonal rutile phase of TiO_2 (JCPDS No.21-1276) and face-centered cubic phases of $Yb_2Ti_2O_7$ (JCPDS No.17-0454) and $Er_2Ti_2O_7$ (JCPDS No. 73-1700). By 1mol% or 2mol% Li^+ codoping, the phase structures of Er^{3+}-Yb^{3+}:TiO_2 do not change, but the main diffraction peak of TiO_2 shifts toward larger angles. Phase transformation happens and a new monoclinic phase of $Li_2Ti_4O_9$ (JCPDS No.33-0832) forms when Li^+ codoping concentration increases to 5mol%, and the diffraction peak intensities of $Li_2Ti_4O_9$ increase gradually while Li^+ increases from 5mol% to 20mol%.

The Li^+ codoping concentration higher than 20mol% results in further increase of diffraction peak intensities of $Li_2Ti_4O_9$ phase. The main diffraction peak of TiO_2 shifts reversely toward smaller angles for Li^+ concentration of 5mol%~20mol%. Substituting the Ti^{4+} ion by the smaller Li^+ ion causes the host lattice to shrink and occupying the interstitial sites causes the host lattice to expand. Consequently, the peak shift toward larger angles by 1mol%~2mol% Li^+ codoping is ascribed to the substitution of Ti^{4+} sites by Li^+ ions, and the peak shift toward smaller angles by 5mol% ~ 20mol% Li^+ codoping is ascribed to the occupation of interstitial sites by Li^+ ions.

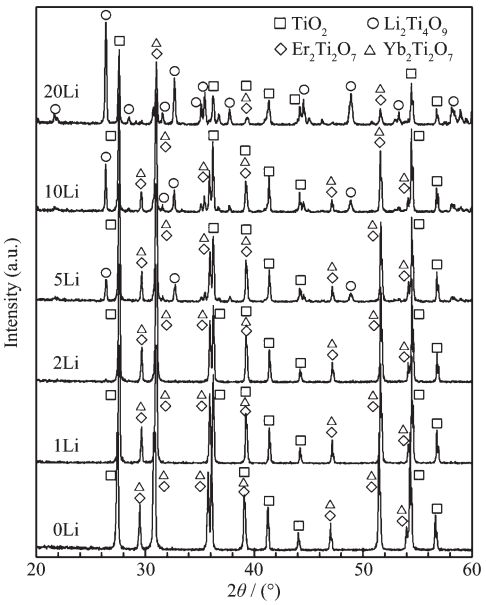

Fig.1 XRD patterns of Er^{3+}-Yb^{3+}:TiO_2 powders codoped with 0mol%~20mol% Li^+

Fig.2 gives the ultraviolet, visible and infrared emissions spectra of 1mol% Er^{3+}-10mol% Yb^{3+} doped TiO_2 by 0, 2mol%, 5mol% and 20mol% Li^+ codoping. The ultraviolet, blue, green and red upconversion and infrared downconversion emissions are observed from the $^4G_{11/2}\rightarrow{}^4I_{15/2}$, $^2H_{9/2}\rightarrow{}^4I_{15/2}$, $^2H_{11/2}/{}^4S_{3/2}\rightarrow{}^4I_{15/2}$, $^4F_{9/2}\rightarrow{}^4I_{15/2}$ and $^4I_{13/2}\rightarrow{}^4I_{15/2}$ transitions of Er^{3+} in the wavelengths of 350~1 700 nm, respectively. The 2mol% Li^+ codoping has no effect on the shape of the emission spectra of Er^{3+}-Yb^{3+}:TiO_2, but uniformly increases the intensities of ultraviolet, visible and infrared emissions. With Li^+ codoping concentration increasing to 5mol%, the shape of emission spectra of Er^{3+}-Yb^{3+}:TiO_2 changes obviously. It can be seen that the ultraviolet, blue and green emissions increases higher than that of red and infrared emissions. The intensities of ultraviolet, visible and infrared emissions are further enhanced significantly by 20mol% Li^+ codoping. For Li^+ codoping concentration higher than 20mol%, we found that the ultraviolet, visible and infrared emissions reached maximum by 25mol% Li^+ codoping and then decreased dramatically with the further increase of Li^+ codoping concentration.

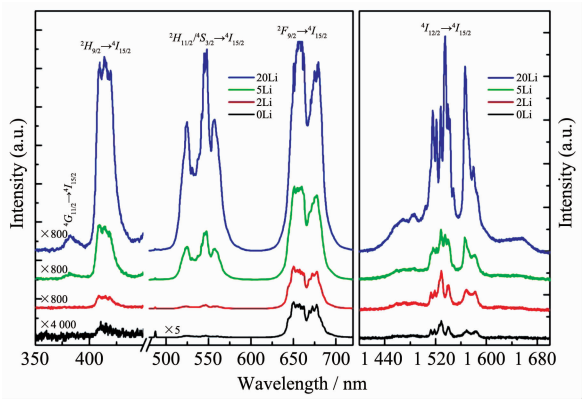

Fig.2 Ultraviolet, visible and infrared emissions spectra of Er^{3+}-Yb^{3+}:TiO_2 by 0, 2, 5 and 20mol% Li^+ codoping

Fig.3 shows the integrated emissions intensities of ultraviolet, visible and infrared emissions of 1mol% Er^{3+} -10mol% Yb^{3+} doped TiO_2 as a function of Li^+ codoping concentration. Due to the upconversion and downconversion emissions are detected by different detectors, the intensities of upconversion emissions cannot be compared with that of downconversion emissions. As shown in Fig.3, the intensities of ultraviolet, visible and infrared emissions dramatically increase with Li^+ codoping concentration of 0mol%~20mol%. It can be observed that the change of intensities of ultraviolet, visible and infrared emissions with Li^+ codoping concentration is divided into two stages. With the Li^+ codoping concentration below 2mol%, the intensities of ultraviolet, blue, green, red and infrared emissions enhance linearly with the Li^+ concentration. When the Li^+ codoping concentration increasing above 5mol%, the ultraviolet, blue and green emissions enhance significantly than the infrared and red emissions. The maximal intensities of ultraviolet, blue, green and red upconversion and infrared

downconversion emissions are obtained for Er^{3+}-Yb^{3+}:TiO_2 by 20mol% Li^+ codoping, which are about 50, 80, 600, 30 and 16 times higher than that of Er^{3+}-Yb^{3+}:TiO_2, respectively.

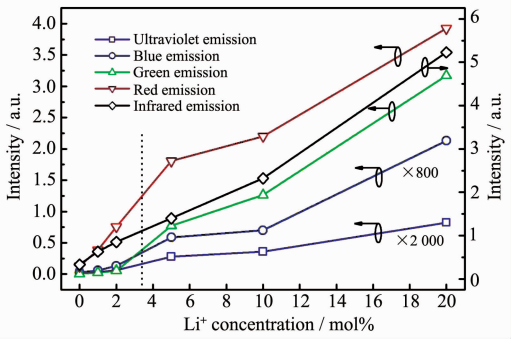

Fig.3　Integrated emissions intensities of ultraviolet, visible and infrared emissions of Er^{3+}-Yb^{3+}:TiO_2 as a function of Li^+ codoping concentration

The schematic energy levels diagram of Er^{3+} and Yb^{3+} as well as the proposed mechanisms for ultraviolet, visible and infrared emissions by a 976 nm LD excitation is given in Fig.4. The green upconversion emission is produced by transitions of $^2H_{11/2}$/$^4S_{3/2}$→$^4I_{15/2}$ of Er^{3+}. The two emitting levels of $^2H_{11/2}$ and $^4S_{3/2}$ are mainly populated by the excited state absorption (ESA (I)), two successive energy transfers ET(I), ET(Ⅲ) and nonradiative decay from $^4F_{7/2}$ to $^2H_{11/2}$ and $^4S_{3/2}$ levels. About the red upconversion emission by transition of $^4F_{9/2}$→$^4I_{15/2}$ of Er^{3+}, the population of $^4F_{9/2}$ level is ascribed mainly to ET(Ⅱ) and the cross-relaxation (CR) process[19]. The Er^{3+} in the $^4S_{3/2}$ level is further promoted to the $^4G_{11/2}$ level through ESA (Ⅱ) process and the ultraviolet emission centered at 382 nm is generated.

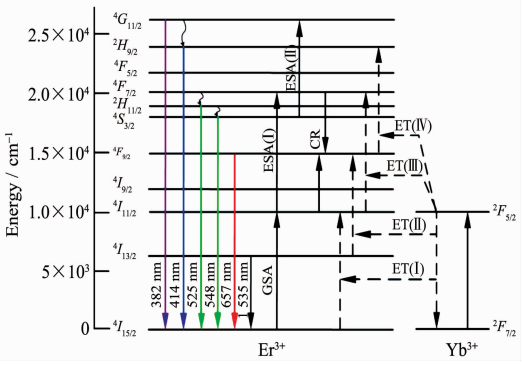

Fig.4　Schematic energy levels diagram of Er^{3+} and Yb^{3+} as well as the proposed mechanisms for ultraviolet, visible and infrared emissions by a 976 nm LD excitation

The nonradiative decay from $^4G_{11/2}$ to $^2H_{9/2}$ and the ET(Ⅳ) process produce the blue emission by the transition of $^2H_{9/2}$→$^4I_{15/2}$. The infrared downconversion emission with broadband extending from 1 400 to 1 700 nm which centered at 1 553 nm is attributed to transition of $^4I_{13/2}$→$^4I_{15/2}$ of Er^{3+}.

The crystal field symmetry of Er^{3+} in the host matrix could affect the intra 4*f* transition probabilities of Er^{3+} and then changed the luminescence efficiency of Er^{3+} doped materials efficiently[9-10]. The phase structures of Er^{3+}-Yb^{3+}:TiO_2 did not change with the dissolving of Li^+ in the matrix by 1mol% or 2mol% Li^+ codoping. Although Li^+ was not energetically strong enough to alter the phase structure, strain created in chemical bonds due to Coulomb interactions was expected to change the length of chemical bond of Er^{3+}. The shift of diffraction peaks of TiO_2 by 1mol% and 2mol% Li^+ codoping in Fig.1 indicated the change of lattice constant, which also showed that the length of chemical bond of Er^{3+} varied with Li^+ codoping. Bai et al. also found that the Er-O bond length in the Er^{3+}:ZnO nanocrystals was altered with the addition of Li^+ by using extended X-ray absorption fine structure spectroscopy (EXAFS)[16]. The length change of the chemical bond of Er^{3+} led to the decrease of local crystal field symmetry around Er^{3+}, inducing the increase of the transition probabilities which govern various intra 4*f* transitions of Er^{3+}[16]. Therefore, both ultraviolet, blue, green and red upconversion and infrared downconversion emissions enhanced uniformly with the shape of emission spectra having no obviously change. Phase transformation happened and a new phase of $Li_2Ti_4O_9$ formed when the codoping concentration of Li^+ increased to 5mol%. The monoclinic phase of $Li_2Ti_4O_9$ was less symmetric than the tetragonal phase of TiO_2, so the crystal field symmetry of Er^{3+} decreased by 5mol% Li^+ codoping. The induced low symmetry of the crystal field of Er^{3+} favored the luminescence emission properties[20]. Therefore, the ultraviolet, visible and infrared emissions enhanced significantly. Due to the crystal field symmetry was different for Er^{3+} in the different crystal phases, the nature of emissions of Er^{3+} from the TiO_2 and $Li_2Ti_4O_9$ phases was not identical. The

increase trends of ultraviolet, visible and infrared emissions by 5mol% Li^+ codoping was no longer uniform as shown in Fig.3. The ultraviolet, blue and green emissions increased more quickly than the red and infrared emissions. With the concentration of Li^+ increased from 5mol% to 20mol%, the increasing content of $Li_2Ti_4O_9$ phase further reduced the symmetry of Er^{3+}, leading to the further enhancement of ultraviolet, visible and infrared emissions.

3 Conclusions

1mol% Er^{3+}-10mol% Yb^{3+} doped TiO_2 powders by 0mol%~20mol% Li^+ codoping have been prepared by sol-gel method. No change of phase structure was observed for Er^{3+}-Yb^{3+} doped TiO_2 by 1mol% or 2mol% Li^+ codoping, while phase transformation happened and a new phase of $Li_2Ti_4O_9$ formed by 5mol%~20mol% Li^+ codoping. The ultraviolet, blue, green and red upconversion and infrared downconversion emissions of Er^{3+}-Yb^{3+}:TiO_2 enhanced significantly by increasing Li^+ from 0mol% to 20mol%. The intensities of ultraviolet, visible and infrared emissions uniformly enhanced by 1mol% and 2mol% Li^+ codoping, which resulted from the distortion of crystal field symmetry of Er^{3+} caused by Li^+ dissolving. The selective increase of ultraviolet to infrared emissions by 5mol%~20mol% Li^+ codoping was ascribed to the variation of the crystal field symmetry of Er^{3+} caused by the phase transformation.

References:

[1] Dosev D, Kennedy I M, Godlewski M, et al. *Appl. Phys. Lett.*, **2006**,**88**(1):011906(3 pages)

[2] Beurer E, Grimm J, Gerner P, et al. *J. Am. Chem. Soc.*, **2006**, **128**(10):3110-3111

[3] De la Posa E, Salas P, Desirena H, et al. *Appl. Phys. Lett.*, **2005**,**87**(24):241912(3 pages)

[4] Dong B, Liu D P, Wang X J, et al. *Appl. Phys. Lett.*, **2007**,**90** (18):181117(3 pages)

[5] LIU Si-Yun(刘四运), XU Sheng(徐晟), PENG Qing(彭卿). *Chinese J. Inorg. Chem.*(*Wuji Huaxue Xuebao*), **2007**,**23**(9): 1657-1661

[6] Judd B R. *Phys. Rev.*, **1962**,**127**(3):750-761

[7] Ofelt G S. *J. Chem. Phys.*, **1962**,**37**(3):511-520

[8] XIA Shang-Da(夏上达). *Chinese J. Lumin.*(*Faguang Xuebao*), **2007**,**28**(4):465-478

[9] Patra A, Friend C S, Kapoor R, et al. *Appl. Phys. Lett.*, **2003**, **83**(2):284-286

[10]Patra A, Friend C S, Kapoor R, et al. *Chem. Mater.*, **2003**,**15** (19):3650-3655

[11]Kozanecki A, Stepikhova M, Lanzerstorfer S, et al. *Appl. Phys. Lett.*, **1998**,**73**(20):2929-2931

[12]Orignac X, Barbier D, Du X M, et al. *Opt. Mater.*, **1999**,**12**(1): 1-18

[13]ZHANG Hong-Bo(张洪波), CUI Guang(崔光), SU Chun-Hui (苏春辉), et al. *Chinese J. Inorg. Chem.*(*Wuji Huaxue Xuebao*), **2010**,**26**(1):144-148

[14]CAO Bao-Sheng(曹保胜), FENG Zhi-Qing(冯志庆), DONG Bin(董斌), et al. *Mater. Rev.*(*Cailiao Daobao*), **2009**,**23**(12): 104-106

[15]Bai Y, Yang K, Wang Y, et al. *Opt. Commun.*, **2008**,**281**(10): 2930-2932

[16]Bai Y, Wang Y, Yang K, et al. *J. Phys. Chem. C*, **2008**,**112** (32):12259-12263

[17]Chen G Y, Liu H C, Liang H J, et al. *Solid State Commun.*, **2008**,**148**(3/4):96-100

[18]Chen G Y, Liu H C, Somesfalean G, et al. *Appl. Phys. Lett.*, **2008**,**92**(11):113114(3 pages)

[19]Vetrone F, Boyer J C, Capobianco J A, et al. *Chem. Mater.*, **2003**,**15**(14):2737-2743

[20]Fornasiero P, Speghini A, Monte R Di, et al. *Chem. Mater.*, **2004**,**16**(10):1938-1944